

Nanostructured GaN: Microstructure and optical properties

M. Benaissa*

Instituto Nacional de Investigaciones Nucleares (ININ), Gerencia de Ciencia de Materiales, Amsterdam 46, Despacho 202, Colonia Hipódromo-Condesa, 06100 México Distrito Federal, Mexico

M. José-Yacamán, J. M. Hernández, and Bokhimi

Instituto de Física-Universidad Nacional Autónoma de México, Apartado Postal 20-364, México Distrito Federal 01000, Mexico

K. E. Gonsalves

Polymer Science Program, Institute of Materials Science, University of Connecticut, Storrs, Connecticut 06269 and Department of Chemistry, University of Connecticut, Storrs, Connecticut 06269

G. Carlson

Department of Chemistry, University of Connecticut, Storrs, Connecticut 06269
(Received 21 June 1996)

In the present study, the microstructure and optical properties of a nanostructured composite that consists of nanocrystalline GaN imbedded in a poly(methyl methacrylate) thin film matrix (GaN/PMMA) are reported. X-ray powder diffraction and high-resolution transmission electron microscopy were performed to analyze the microstructure, while the optical properties were measured by optical absorption and photoluminescence. Microstructural analyses showed that GaN nanocrystallites imbedded in the PMMA matrix have a size of about 5.5 nm, and crystallize in the zinc-blende lattice (the lattice constant $a_0 \sim 0.45$ nm) with a considerable fraction of structural defects such as nitrogen vacancies and stacking faults. Optical-absorption measurements indicate that the band-gap energy of the GaN/PMMA composite is approximately 3.51 eV. [S0163-1829(96)01148-4]

I. INTRODUCTION

Gallium nitride (GaN) and related III-V nitrides have recently attracted extensive experimental and theoretical interest due to their physical properties, such as a wide and direct band gap,¹ low compressibility, and high thermal conductivity, which make them strong candidates for short-wavelength electroluminescent devices and high-temperature/high power diodes and transistors.^{2,3} The development of the III-V nitride-based technology requires continuous advances in material preparation and device processing technology. Thin-film preparation techniques have already shown a successful realization of high quality GaN films, demonstrating bright light-emitting diodes (LED's) (Ref. 4) and short-wavelength laser-diodes (LD's) (Ref. 5) in blue and blue-green regions. Particular interest is currently centered on advanced chemical synthetic routes for producing a size-controlled nanocrystalline GaN semiconductor.⁶ This latter will continue to emit more efficiently due to its direct electronic transition. Interestingly, in growing a reduce-sized semiconductor distributed in an optically transparent matrix, quantum-size effects are reported to be very important.⁷ In such composites, in addition to a possible increase of the band-gap energy accompanied by a shift of excitons to higher energies owing to quantum confinement effects, one also would expect an enhancement in the third-order nonlinear optical susceptibility (χ^3).⁸ For these reasons, quantum-dot composites are a promising future semiconducting device material. In this study, we report the microstructure and optical properties of a nanostructured composite that consists of nanocrystalline GaN imbedded in a poly(methyl methacrylate) thin film matrix.

II. EXPERIMENT

Synthesizing GaN semiconductors through a chemical process was achieved decades ago.^{9,10} However, only recently, success in preparing good-quality nanosized GaN through chemical processes was demonstrated.^{6,11} The nanostructured GaN used in this work was prepared by reacting $\text{LiN}(\text{CH}_3)_2$ with GaCl_3 in hexane at room temperature to obtain the aminogallane precursor $\text{Ga}_2[\text{NMe}_2]_6$. This product was filtered, crystallized, and purified by vacuum sublimation. The aminogallane was decomposed under flowing ammonia gas for 4 h at 600 °C. The resulting grayish solid was stored and handled under an inert atmosphere to prevent oxidation. This sample will be denoted as nano-GaN. Part of the latter (60 mg) was mixed with 1 ml of methylmethacrylate, then sonicated, decanted, and thermally polymerized at 72 °C for 50 min. This sample will be denoted as a GaN/PMMA composite. A detailed description of the synthesis is reported elsewhere.⁶ The crystalline structure of both samples was analyzed by x-ray powder diffraction using a Siemens D-5000 diffractometer equipped with a $\text{Cu}(K\alpha)$ radiation source and a graphite monochromator. The intensity was determined by step scanning in the 10° – 130° range, with a 2θ step of 0.02° each 3 s. The crystalline structure of the compounds was refined using the Rietveld technique as described in the new version of the DBWS-9411 program.¹² The profile-breadth fitting was determined considering the averaged crystallite size and crystal-microstrain parameters using the pseudo-Voigt function as modified by Thompson, Cox, and Hastings.¹³ High-resolution transmission electron microscopy (HRTEM) was performed, using a JEM4000EX

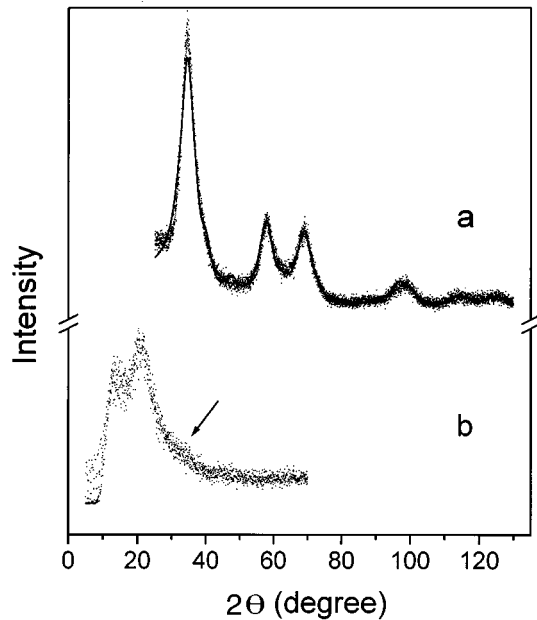


FIG. 1. (a) X-ray-diffraction pattern of nano-GaN. Dots illustrate experimental data, while the solid line shows the pattern obtained from the Rietveld refinement ($R_{wp}=0.103$). The refined pattern was obtained by mixing cubic ($R_{FC}=0.008$) and hexagonal ($R_{FH}=0.009$) GaN phases. (b) X-ray-diffraction pattern corresponding to the GaN/PMMA composite. (R_{wp} : residual considering the whole pattern; R_{FC} : residual considering factor structures of cubic GaN; R_{FH} : residual considering factor structures of hexagonal GaN).

electron microscope operated at 400 keV, for both samples. For nano-GaN, the sample was prepared by simply grinding the powder between two glass plates, and bringing the fine powder into contact with a holey carbon-coated copper TEM grid under a nitrogen atmosphere. In the case of the GaN/PMMA composite, the specimen was embedded in epoxy resin, and sliced down to a thickness of about 80 nm using a LKB Ultratome V equipped with a diamond knife. The slices were then picked up onto a carbon-coated copper TEM grid. Absorption measurements were obtained with a Perkin-Elmer Model 330 double-beam spectrophotometer, and photoluminescence (PL) measurements were performed using the third-harmonic frequency of a pulsed Nd:YAG (yttrium aluminum garnet) laser (355 nm) as an excitation source and a photon counter detector.

III. RESULTS AND DISCUSSION

Experimental (dots) and theoretical (solid line) x-ray-diffraction patterns are presented in Fig. 1(a) obtained from nano-GaN. The pattern clearly exhibits the $\{111\}$, $\{220\}$, and $\{311\}$ reflections of the metastable cubic GaN phase, known earlier as the sphalerite structure¹⁴ and later as zinc blende,¹⁵ at angles 2θ of 35.5° , 58° , and 69° , respectively. The asymmetry of the first reflection can be interpreted as an overlapping of the $\{111\}$ and a confined $\{002\}$ of weak intensity. X-ray refinement using the Rietveld method shows that the best match with experiment is obtained when considering a structure that is a mixture of zinc blende (zb) and wurtzite (w) GaN phases, with a particle size determined from the

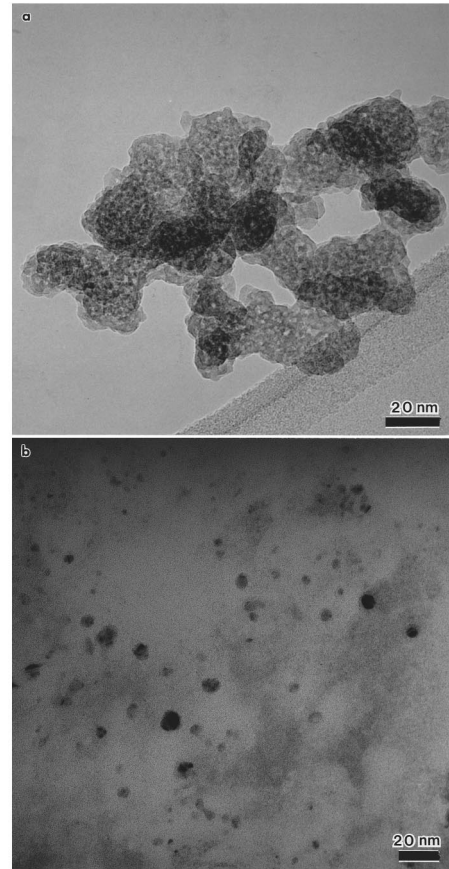


FIG. 2. Typical low-magnification HRTEM micrographs showing the microstructure of the (a) nano-GaN powder and in the (b) GaN/PMMA composite.

coherence length calculated from the Debye-Scherrer formula of about 2.8 ± 0.3 nm. In fact, the simulation considers that each particle consists of a majority [76.7(6)%] of zb-GaN mixed with a smaller amount [23.3(4)%] of w-GaN in such a way that the $\langle 111 \rangle$ GaN_{zb} crystallographic axis is parallel to the $\langle 0001 \rangle$ GaN_w axis. This result suggests that nano-GaN particles mainly crystallize in the zb lattice, with some stacking disorder along the $\langle 111 \rangle$ axis. The lattice constant $a_{\text{nano-GaN}}$ deduced from our x-ray Rietveld refinement is $0.4500(2)$ nm, which is consistent with measurements previously reported. The x-ray pattern corresponding to the GaN/PMMA composite is shown in Fig. 1(b), indicating two low-angle reflections originating from a high range order within the PMMA polymer matrix, along with a shoulder (arrow) at $2\theta=35.5^\circ$ attributed to the $\{111\}$ reflection of GaN. Because the signal-to-noise was too weak, no refinement was performed. Preliminary chemical analyses⁶ of the as-synthesized GaN showed a nitrogen-poor material (Ga:N=1:0.86) that contains traces of carbon (0.8 wt %) and hydrogen (0.5 wt %). Thermodynamically, a Ga interstitial should be much more difficult to form in a zb-GaN than a N vacancy. Thus, it is reasonable to assume that the GaN nonstoichiometry is due to N vacancies.

Typical low-magnification electron micrographs of nano-GaN and GaN/PMMA are shown in Figs. 2(a) and 2(b), respectively. An overview of the former [Fig. 2(a)] shows large porous particles of about 30 nm in size. A highly magnified image [Fig. 3(a)] indicates that each of these large

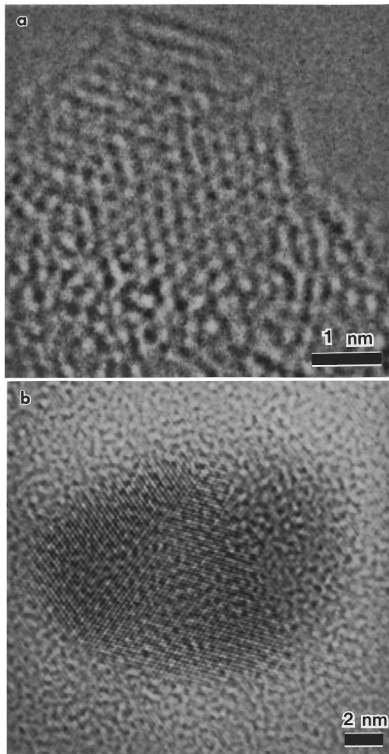


FIG. 3. HRTEM micrographs showing the atomic structure of the nanostructured GaN crystallites in the (a) nano-GaN powder and in the (b) GaN/PMMA composite.

particles is actually composed of small agglomerated crystallites, each about 3 nm in size, in accordance with the value deduced from the above x-ray data. In return, the GaN/PMMA composite [Fig. 3(b)] shows highly dispersed GaN crystallites with an average size around 5.5 nm,⁶ which is slightly higher than that in nano-GaN, partly due to the incorporation process and the deagglomeration mechanism of the nanocrystallites within the polymer matrix. Examination of the crystallite structure in both samples [Figs. 3(a) and 3(b)] shows that structural defects are very abundant. Indeed, close analysis of the atomic structure in nano-GaN [Figs. 4(a) and 4(b)] indicates very short-range order and a considerable number of stacking faults. Particularly in Fig. 4(b), a typical stacking fault is illustrated in which the change in the stacking can be regarded as a formation of *w*-GaN nanodomain. This result, on one hand, confirms the mixture of the *zb*- and *w*-GaN structures considered in our x-ray analyses, and, on the other hand, would explain the asymmetry observed in the first x-ray reflection [see Fig. 1(a)]. In addition one can notice that the order range is higher in the GaN/PMMA; in other words, the incorporation of nano-GaN in the polymer remarkably reduces the stacking disorder density. At this stage, it is not clear whether the reduction of the disorder is due to the increase of the nanocrystallite size, or to the surrounding polymer that would stabilize the termination of the nanocrystallites or to both effects. Figures 5(a) and 5(b), respectively, show the kind of defects encountered in the GaN/PMMA composite, namely, twins and stacking faults. Generally, stacking faults are structural features that have widely been reported to exist in *zb*-GaN (Refs. 11, 14, and 15) and in most zinc-blende III-V analogues. Normally, GaN crystallizes in the wurtzite crystal structure. At rela-

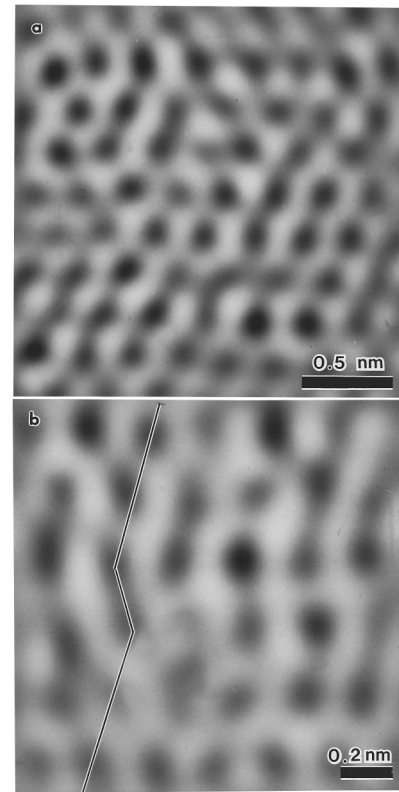


FIG. 4. High-magnification HRTEM showing structural defects in the nanocrystalline GaN sample. Note the high density of the stacking disorder. Apparently, the disorder in the micrograph (a) is bidimensional, while in (b) the disorder is one dimensional.

tively low temperatures, the high density of stacking defects would enable the *zb*-GaN structure to be dominant. A transition to the *w*-GaN phase might be expected at high temperatures. Generally, a lack of high-quality *zb*-GaN in fact explains the reason why most of the interest was focused on the *w*-GaN thin films (partly due to the presence of adequate substrates), although cubic GaN should theoretically¹⁶ exhibit superior electronic properties because of the isotropy of its lattice.

Figure 6 shows the optical-absorption spectrum obtained at room temperature from the GaN/PMMA composite. The energy gap was determined to be 3.51 eV by fitting¹⁷ our experimental data for the absorption coefficient from 250 to 475 nm. As expected, this value is slightly larger than those previously reported for *zb*-GaN (3.45 eV [Ref. 15(b)] and 3.2 eV (Ref. 18)). The shift to higher energies observed in the optical absorption suggests that quantum confinement is taking place. Also, the spectrum exhibits an exciton absorption feature (3.73 eV) near the absorption edge (see the arrow and inset in Fig. 6). The exciton and band-gap energies actually reported are in good agreement with their dependence on the size distribution of the GaN nanocrystallites as tested using the effective-mass approximation.^{7,19,20} The photoluminescence spectrum obtained from GaN/PMMA gave results thought to be a mixture of various electronic events, although an emission in the blue region was clearly obtained.⁶ The information derived from luminescence obtained from zero-dimensional (0D) systems often tends to be more complex than that from absorption. In this context, one of the

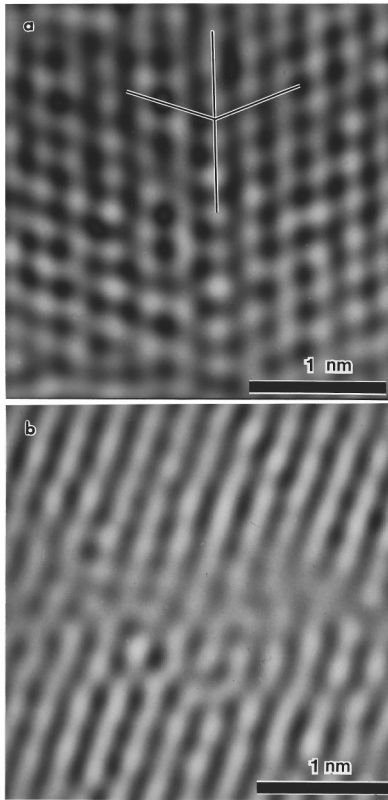


FIG. 5. High-magnification HRTEM showing, respectively, (a) a twin and (b) stacking faults observed in the GaN/PMMA composite.

parameters that can affect the luminescence profile is the shape of the nanocrystallites. The majority of the models used in the literature to calculate energy levels for 0D systems usually assume spherical shapes for ease of calculation. In the case of a zb-GaN structure, the shape of the nanocrystals can be assumed to be spherical if they are free of stacking disorder. The shape would adopt a configuration in which the GaN nanocrystallite grows along the four equivalent fast $\langle 111 \rangle$ growth directions. If stacking faults occur along one of those $\langle 111 \rangle$ directions, as demonstrated in the HRTEM images, the nanocrystallite will tend to grow longer in the stacking fault direction, resulting in a departure from a spherical shape. In these circumstances, one can use the spherical approximation for the absorption spectra description,²¹ but the luminescence is expected to differ sig-

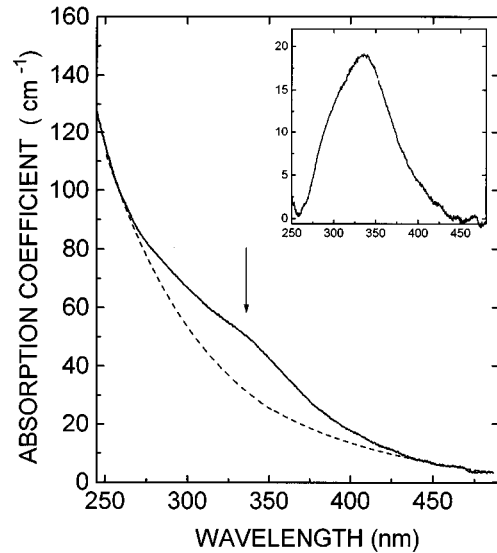


FIG. 6. Optical-absorption spectrum obtained at room temperature from the GaN/PMMA composite. The inset shows the exciton absorption feature obtained as the difference between experimental data and the fitting to the absorption edge (dashed line).

nificantly for nonspherical shapes. Furthermore, extra features observed in the luminescence spectrum obtained from GaN/PMMA probably originate from surface states associated with nanocrystallite termination and changes in the potential due to structural defects and N vacancies. Further studies are needed to fully interpret our luminescence results.

IV. CONCLUSION

In summary, we have presented a study on the microstructure and optical properties of a nanocrystalline GaN imbedded in a poly(methyl methacrylate) thin-film matrix. The nanocrystalline size distribution was found to be centered around 5.5 nm. The GaN structure within the composite was found to crystallize in the zinc-blende lattice (the lattice constant close to 0.45 nm) with a considerable fraction of structural defects such as N vacancies and stacking faults. The optical-absorption measurements indicate that the band-gap energy is 3.51 eV.

ACKNOWLEDGMENT

We thank L. Rendon (UNAM) for his technical help.

*Corresponding author. Electronic address: mohamed@sysu11.ifisicacu.unam.mx

¹H. P. Maruska and J. J. Tietjen, *Appl. Phys. Lett.* **15**, 327 (1969).

²S. Strite and H. Morkoç, *J. Vac. Sci. Technol. B* **10**, 1237 (1992).

³S. Strite, M. E. Lin, and H. Morkoc, *Thin Solid Films* **231**, 197 (1993).

⁴S. Nakamura, T. Mukai, and M. Senoh, *Appl. Phys. Lett.* **64**, 1687 (1994).

⁵S. Nakamura, M. Senoh, S. I. Nagahama, N. Iwasa, T. Yamada, T. Matsushita, H. Kiyoku, and Y. Sugimoto, *Jpn. J. Appl. Phys. B* **35**, L74 (1996).

⁶K. E. Gonsalves, G. Carlson, S. P. Rangarajan, M. Benaissa, and M. José-Yacamán, *J. Mater. Chem.* **6**, 1451 (1996).

⁷For a comprehensive review of low-dimensional systems, see A. D. Yoffe, *Adv. Phys.* **42**, 173 (1993).

⁸L. Brus, *Appl. Phys. A* **53**, 465 (1991).

⁹W. C. Johnson, J. P. Parsons, and M. C. Crew, *J. Phys. Chem.* **36**, 2651 (1932).

¹⁰H. G. Grimmeiss and H. Koelmans, *Z. Naturforsch.* **14a**, 264 (1959).

¹¹J. W. Hwang, J. P. Campbell, J. Kozubowski, S. A. Hanson, J. F. Evans, and W. L. Gladfelter, *Chem. Mater.* **7**, 517 (1995).

¹²R. A. Young, A. Sakthivel, T. S. Moss, and C. O. Paiva-Santos, *J. Appl. Crystallogr.* **28**, 366 (1995).

¹³P. Thompson, D. E. Cox, and J. B. Hastings, *J. Appl. Crystallogr.* **20**, 445 (1974).

- ¹⁴W. Seifert and A. Tempel, *Phys. Status Solidi A* **23**, K39 (1974).
- ¹⁵(a) M. J. Paisley, Z. Sitar, J. B. Posthill, and R. F. Davis, *J. Vac. Sci. Technol. A* **7**, 701 (1989); (b) S. Strite, J. Ruan, Z. Li, A. Salvador, H. Chen, D. J. Smith, W. J. Choyke, and H. Morkoç, *ibid.* **9**, 1924 (1991).
- ¹⁶K. Das and D. K. Ferry, *Solid-State Electron.* **19**, 851 (1976).
- ¹⁷E. D. Palik, *Handbook of Optical Constants of Solids* (Academic, London, 1985).
- ¹⁸T. Lei, T. D. Moustakas, R. J. Graham, Y. He, and S. J. Berkowitz, *J. Appl. Phys.* **71**, 4933 (1992).
- ¹⁹L. E. Brus, *IEEE J. Quantum Electron.* **QE-22** 1909 (1986).
- ²⁰Y. Kayanuma, *Phys. Rev. B* **38**, 9797 (1988).
- ²¹Al. L. Efros and A. V. Rodina, *Phys. Rev. B* **47**, 10 005 (1993).